Acta Pharmaceutica Sinica B 2018;8(6):933–943

Chinese Pharmaceutical Association
Institute of Materia Medica, Chinese Academy of Medical Sciences

Acta Pharmaceutica Sinica B

www.elsevier.com/locate/apsb
www.sciencedirect.com

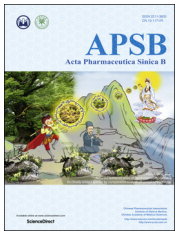

ORIGINAL ARTICLE

Sulfur-enriched alkaloids from the root of *Isatis indigotica*

Qinglan Guo[a], Chengbo Xu[a], Minghua Chen[a,b], Sheng Lin[a], Yuhuan Li[b], Chenggen Zhu[a], Jiandong Jiang[a,b], Yongchun Yang[a], Jiangong Shi[a,*]

[a]*State Key Laboratory of Bioactive Substance and Function of Natural Medicines, Institute of Materia Medica, Chinese Academy of Medical Sciences & Peking Union Medical College, Beijing 100050, China*
[b]*Institute of Medicinal Biotechnology, Chinese Academy of Medical Sciences & Peking Union Medical College, Beijing 100050, China*

Received 8 June 2018; received in revised form 3 August 2018; accepted 9 August 2018

KEY WORDS

Cruciferae;
Isatis indigotica;
Sulfur-containing alkaloids;
Isatithioetherins A–E;
Isatithiopyrins A and B;
Isoepigoitrin;
Isogoitrin;
Antiviral activity

Abstract Five new sulfur-enriched alkaloids isatithioetherins A–E (**1**–**5**), and two pairs of scalemic enantiomers (+)- and (−)-isatithiopyrin B (**6a** and **6b**) and isoepigoitrin and isogoitrin (**7a** and **7b**), along with the known scalemic enantiomers epigoitrin and goitrin (**8a** and **8b**), were isolated and characterized from an aqueous extract of the *Isatis indigotica* roots. Their structures were determined by extensive spectroscopic data analysis, including 2D NMR and theoretical calculations of electronic circular dichroism (ECD) spectra based on the quantum-mechanical time-dependent density functional theory (TDDFT). Compounds **1**–**5** represent a novel group of sulfur-enriched alkaloids, biogenetically originating from stereoselective assemblies of epigoitrin-derived units. Isolation and structure characterization of **6a** and **6b** support the postulated biosynthetic pathways for the diastereomers **9a** and **9b** *via* a rare thio-Diels–Alder reaction. Compounds **2** and **4** showed antiviral activity against the influenza virus A/Hanfang/359/95 (H3N2, IC_{50} 0.60 and 1.92 μmol/L) and the herpes simplex virus 1 (HSV-1, IC_{50} 3.70 and 2.87 μmol/L), and **2** also inhibited Coxsackie virus B3 (IC_{50} 0.71 μmol/L).

*Corresponding author.
E-mail address: shijg@imm.ac.cn (Jiangong Shi).

Peer review under responsibility of Institute of Materia Medica, Chinese Academy of Medical Sciences and Chinese Pharmaceutical Association.

https://doi.org/10.1016/j.apsb.2018.08.005

1. Introduction

The dried roots and leaves of *Isatis indigotica* Fort. (Cruciferae), having names of "ban lan gen" and "da qing ye", respectively, are used in traditional Chinese medicine for the treatment of various diseases. They are among the most common ingredients of formulations used for treating influenza, cold, and fever[1]. Chemical and pharmacological studies demonstrated that extracts of these drug materials contained diverse chemical constituents with various biological activities[2–24]. Although the drug materials are practically utilized by decocting with water, only few chemical studies on the water decoctions were previously reported[18–24]. Because the constituents of extracts are highly dependent upon extraction methods, we consider that there must be unknown bioactive chemical constituents in the decoctions. Therefore, the water decoction of the *I. indigotica* roots was investigated as part of a program to assess the chemical and biological diversity of traditional Chinese medicines[25–47]. This has led to discovery of many new chemical constituents with diverse structural types and biological activities from "ban lan gen"[48–61]. A continuation on the same decoction has resulted in structure characterization of nine new sulfur-containing natural products (**1**−**5**, **6a**, **6b**, **7a**, and **7b** Fig. 1). Among them, **1**–**5** possess unusual sulfur-enriched structures, biogenetically associated with the co-occurring epigoitrin (**8a**, Fig. 1). The enantiomers **6a** and **6b** are diastereomers of **9a** and **9b** (Fig. 1) possessing the unique indolin-2-one, dihydrothiopyran, and 1,2,4-thiadiazole ring system previously reported from the same extract[49] and recently synthesized *via* a rare thio-Diels–Alder reaction[62]. Herein, we report isolation, structure elucidation, and proposed biosynthetic relationship of the new isolates, along with antiviral activities of **2** and **4**.

2. Results and discussion

Compound **1**, a colorless gum with $[\alpha]_D^{20}$ +38.8 (*c* 0.1, MeCN), showed IR absorptions attributable to amino (3208 cm^{-1}), carbonyl (1702 cm^{-1}), and thiocarbonyl (1542 cm^{-1}) functionalities. Its molecular formula was determined as $C_{20}H_{26}N_4NaO_4S_3$ by HR-ESI-MS and NMR spectroscopic data. The ^1H NMR spectrum of **1** showed partially overlapping resonances attributable to a pair of exchangeable amino protons at δ_H 9.57 and 9.62 (each 1H, brs); a pair of disubstituted double bonds at δ_H 5.71 and 5.70 (each 1H, t, J = 5.0 Hz, H-2′ and H-3′) and 5.59 and 5.58 (each 1H, t, J = 6.0 Hz, H-2‴ and H-3‴); and a pair of terminal double bonds at δ_H 5.53 (2H, d, J = 17.5 Hz, H-7a/7″a), 5.42 (2H, d, J = 10.0 Hz, H-7b/7″b), 6.10 and 6.09 (each 1H, ddd, J = 17.5, 10.0, and 8.0 Hz, H-6 and H-6″). In addition, the spectrum displayed partially overlapping resonances assignable to a pair of heteroatom-bearing methines at δ_H 5.34 (2H, dt, J = 10.0 and 8.0 Hz, H-5/5″) and three pairs of heteroatom-bearing methylenes at δ_H 4.47 (2H, t, J = 10.0 Hz, H-4a/4″a), 4.02 and 4.01 (1H each, dd, J = 10.0 and 8.0 Hz, H-4b and H-4″b); 3.98 (2H, t, J = 6.0 Hz, H_2-4‴) and 3.94 (2H, t, J = 5.0 Hz, H_2-4′); 3.23 (2H, d, J = 6.0 Hz, H_2-1‴) and 3.14 (2H, d, J = 5.0 Hz, H_2-1′). The ^{13}C NMR and DEPT spectra exhibited partially overlapping carbon signals corresponding to the above units as well as those due to two pairs of quaternary carbons at δ_C 186.4 (C-2/2″) and 152.0 (C-5′/5‴). Especially differences of the chemical shifts for most of the pairing signals were less than $\Delta\delta_C$ ±0.1. As compared with those of the reported compounds from this plant[48–61], these spectroscopic data suggested that **1** was an unusual asymmetric dimer of alkaloid containing three sulfur atoms, of which the structure was further elucidated by 2D NMR data analysis.

The proton and proton-bearing carbon resonances in the NMR spectra were assigned by the HSQC experiment of **1**. In the ^1H–^1H COSY spectrum, the vicinal coupling cross-peaks of H_2-4/H-5/H-6/H_2-7 (H_2-4″/H-5″/H-6″/H_2-7″) and the HMBC correlations from H_2-4 to C-2, C-5, and C-6 (H_2-4″ to C-2″, C-5″, and C-6″) (Fig. 2), in combination with comparison of the chemical shifts of these proton and carbon signals with those of the co-occurring epigoitrin (**8a**), revealed the presence of a pair of *N*- and *N*″-substituted epigoitrin units in **1**. In addition, the ^1H–^1H COSY cross-peaks of H_2-1′/H-2′/H-3′/H_2-4′/N′*H* and H_2-1‴/H-2‴/H-3‴/H_2-4‴/N‴*H*, together with the HMBC correlations from H_2-1′ to C-1‴ and from H_2-1‴ to C-1′ as well as their chemical shifts, indicated that there were a pair of *N*′- and *N*‴-substituted 4′-amino-but-2′-enyl and 4‴-amino-but-2‴-enyl units, connecting each other *via* a thioether bond between C-1′ and C-1‴. Moreover, the HMBC spectrum of **1** exhibited the correlations from both H_2-4′ and H_2-4‴ to the carbon resonance at δ_C 152.0 (C-5′ and C-5‴). This demonstrated that the amino groups of the sulfur-bridged bis-butenamine moiety must connect *via* C-5′ and C-5‴ with the two epigoitrin units to match requirement of the molecular

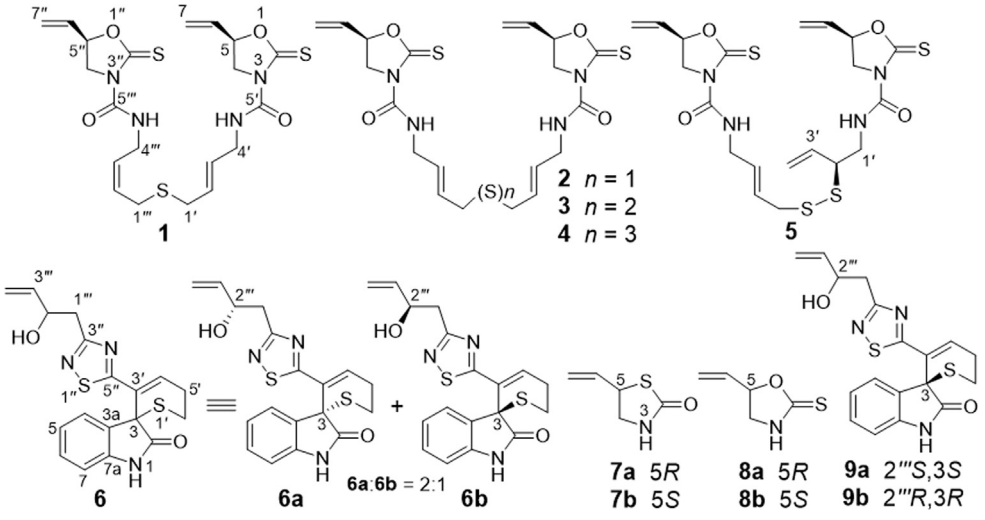

Figure 1 The structures of compounds **1**–**9**.

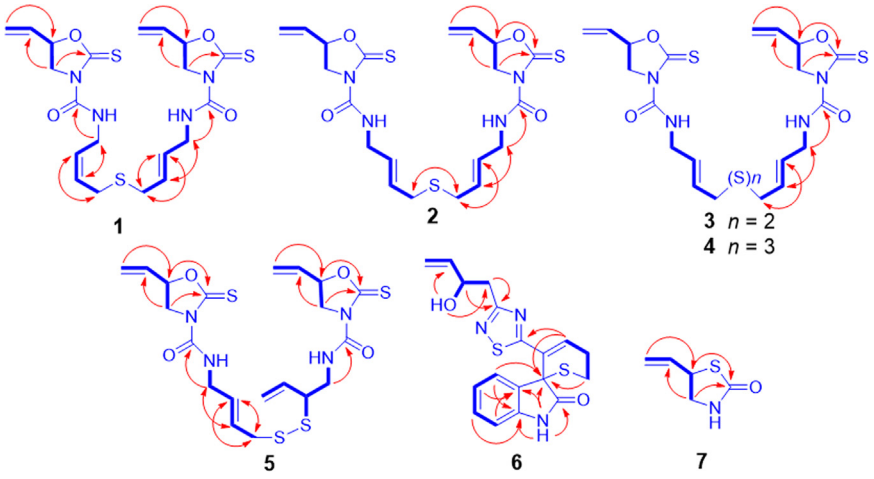

Figure 2 Main ^{1}H–^{1}H COSY (thick lines) and three-bond HMBC (arrows, from ^{1}H to ^{13}C) correlations of compounds **1**–**7**.

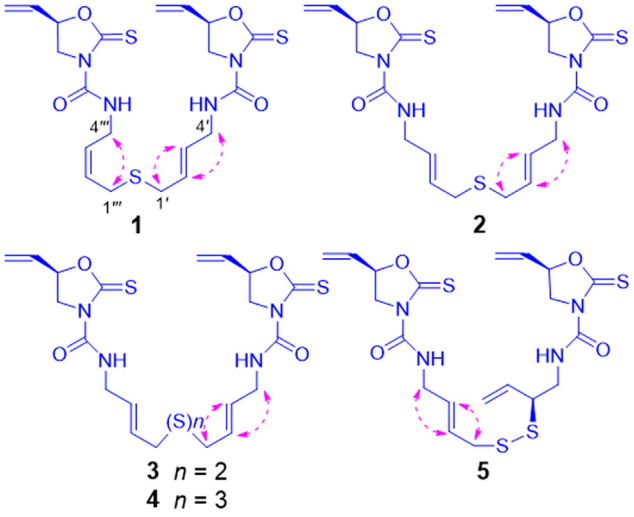

Figure 3 ROESY/NOESY correlations (double arrows between protons) of compounds **1**–**5**.

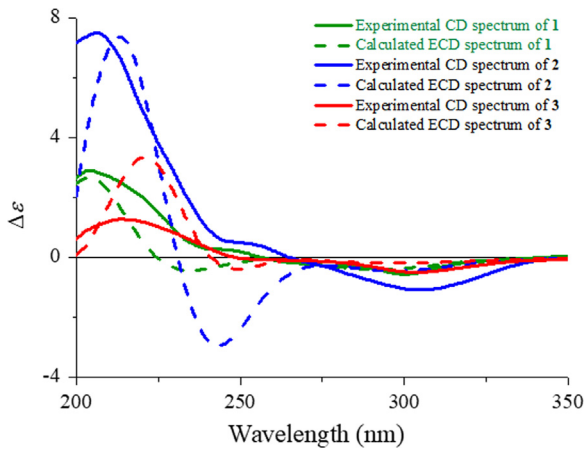

Figure 4 The overlaid experimental CD (full lines) and calculated ECD spectra (dash lines) of compounds **1**–**3**.

formula and *N*- and *N*′′-substitution, though no three-bond correlations from H_2-4 and/or H_2-4′′ to C-5′ and C-5′′′ were observed in the HMBC spectrum. Accordingly, the planar structure of **1** was determined as shown.

The ROESY spectrum of **1** displayed the NOE correlations between H_2-1′′′ and H_2-4′′′ as well as between H_2-1′ and H-3′ and between H-2′ and H_2-4′ (Fig. 3), suggesting a 2′-*trans*-2′′′-*cis* geometric configuration for **1**. The suggestion was supported by the chemical shift rule for the *α*-alkyl carbons connecting to the *trans*- and *cis*-double bonds ($\delta_{trans} > \delta_{cis}$),[63] because the chemical shift values of C-1′ and C-4′ (δ_C 32.9 and 42.2) were larger than those of C-1′′′ and C-4′′′ (δ_C 27.5 and 37.9) in **1**. The specific rotation value of **1** was almost doubled as compared with that of **8a**, $[\alpha]_D^{20}$ +21.6 (*c* 2.4, $CHCl_3$), suggesting that the absolute configuration at C-5 and C-5′′ in **1** are identical to that in **8a**. This was further supported by comparison of the experimental CD and calculated ECD spectra of **1** (Fig. 4). Therefore, the structure of compound **1** was determined and named isatithioetherin A.

Compound **2**, a colorless gum with $[\alpha]_D^{20}$ +32.0 (*c* 1.7, MeCN), showed similar spectroscopic data to those of **1**, except that the NMR spectra of **2** displayed only half the number of resonances corresponding to the proton and carbon atoms expected from the molecular formula. This suggested that **2** was an isomer of **1** with the symmetric structure, which was supported by EI-MS data of **2** at *m/z* (%) 129 (100) and 225 (22) arising from cleavage of the carbamide and thioether bonds, respectively (Supplementary Information Fig. S30). Comparison of the spectroscopic NMR data between **2** and **1** (Table 1) demonstrated that the 2′′′-*cis* double bond in **1** was absent in **2**. Thus, **2** was assigned as the 2′′′-*trans* isomer of **1**, which was proved by 2D NMR data analysis, especially by the HMBC correlation from H_2-1′ to C-1′′′ (H_2-1′′′ to C-1′) and the NOESY correlations between H_2-1′ and H-3′ (H_2-1′′′ and H-3′′′) and H-2′ and H_2-4′ (H-2′′′ and H_2-4′′′) (Figs. 2 and 3) as well as the chemical shifts of C-1′ and C-4′ (C-1′′′ and C-4′′′). The similarity of specific rotation and CD data between **2** and **1** indicated that the two compounds had the same absolute configuration, which was supported by comparison of the experimental CD and calculated ECD spectra of **2** (Fig. 4). Thus, the structure of compound **2** was determined and named isatithioetherin B.

Compound **3** was obtained as a colorless gum with $[\alpha]_D^{20}$ +30.4 (*c* 0.2, MeCN). Its molecular formula $C_{20}H_{26}N_4O_4S_4$ with one more sulfur atom than **1** and **2** was determined by HR-ESI-MS and NMR spectroscopic data. The UV, IR, and NMR spectroscopic

Table 1 NMR spectroscopic data for compounds **1**−**5**[a].

No.	**1**		**2**		**3**		**4**		**5**	
	δ_H	δ_C	δ_H	δ_C	δ_H	δ_C	δ_H	δ_C	δ_H	δ_C
2		186.4		186.4		186.4		186.3		186.4
4a	4.47 t (10.0)	52.5	4.47 dd (11.0, 9.0)	52.5	4.47 dd (11.0, 9.0)	52.5	4.47 dd (11.0, 9.0)	52.5	4.47 dd (11.0, 9.0)	52.5
4b	4.02 dd (10.0, 8.0)		4.00 dd (11.0, 8.0)		4.00 dd (11.0, 8.0)		4.00 dd (11.0, 8.0)		4.00 dd (11.0, 8.0)	
5	5.34 dt (10.0, 8.0)	80.3	5.35 dt (9.0, 8.0)	80.3	5.35 dt (9.0, 8.0)	80.3	5.35 dt (9.0, 8.0)	80.2	5.35 dt (9.0, 8.0)	80.3
6	6.10 ddd (17.5, 10.0, 8.0)	134.5	6.09 ddd (17.5, 10.5, 8.0)	134.5	6.09 ddd (17.5, 10.5, 8.0)	134.5	6.08 ddd (17.0, 10.5, 8.0)	134.5	6.08 ddd (17.0, 10.5, 8.0)	134.5
7a	5.53 d (17.5)	121.0	5.53 d (17.5)	121.0	5.53 d (17.5)	121.0	5.53 d (17.0)	121.0	5.53 d (17.0)	121.0
7b	5.42 d (10.0)		5.43 d (10.5)		5.42 d (10.5)		5.42 d (10.5)		5.42 d (10.5)	
1′a	3.14 d (5.0)	32.9	3.11 d (6.0)	32.3	3.37 d (6.0)	41.3	3.58 d (5.5)	40.9	3.74 dt (12.0, 7.0)	43.6
1′b	3.14 d (5.0)		3.11 d (6.0)		3.37 d (6.0)		3.58 d (5.5)		3.57 dt (12.0, 7.0)	
2′	5.70 t (5.0)	129.6	5.65 t (6.0)	129.6	5.73 t (6.0)	128.1	5.79 t (5.5)	127.4	3.68 q (7.0)	53.5
3′	5.71 t (5.0)	129.5	5.65 t (6.0)	129.5	5.73 t (6.0)	130.9	5.79 t (5.5)	131.5	5.76 ddd (17.0, 10.5, 7.0)	136.2
4′a	3.94 t (5.0)	42.2	3.93 t (6.0)	42.2	3.96 t (6.0)	42.2	3.98 t (5.5)	42.2	5.30 d (17.0)	119.3
4′b	3.94 t (5.0)		3.93 t (6.0)		3.96 t (6.0)		3.98 d (5.5)		5.23 d (10.5)	
5′		152.0		151.7		151.7		151.7		152.0
2″		186.4		186.4		186.4		186.3		186.3
4″a	4.47 t (10.0)	52.5	4.47 dd (11.0, 9.0)	52.5	4.47 dd (11.0, 9.0)	52.5	4.47 dd (11.0, 9.0)	52.5	4.47 dd (11.0, 9.0)	52.5
4″b	4.01 dd (10.0, 8.0)		4.00 dd (11.0, 8.0)		4.00 dd (11.0, 8.0)		4.00 dd (11.0, 8.0)		4.00 dd (11.0, 8.0)	
5″	5.34 dt (10.0, 8.0)	80.3	5.35 dt (9.0, 8.0)	80.3	5.35 dt (9.0, 8.0)	80.3	5.35 dt (9.0, 8.0)	80.2	5.35 dt (9.0, 8.0)	80.3
6″	6.09 ddd (17.5, 10.0, 8.0)	134.5	6.09 ddd (17.5, 10.5, 8.0)	134.5	6.09 ddd (17.5, 10.5, 8.0)	134.5	6.08 ddd (17.0, 10.5, 8.0)	134.5	6.08 ddd (17.0, 10.5, 8.0)	134.5
7″a	5.53 d (17.5)	121.0	5.53 d (17.5)	121.0	5.53 d (17.5)	121.0	5.53 d (17.0)	121.0	5.53 d (17.0)	121.0
7″b	5.42 d (10.0)		5.43 d (10.5)		5.42 d (10.5)		5.42 d (10.5)		5.42 d (10.5)	
1‴	3.23 d (6.0)	27.5	3.11 d (6.0)	32.3	3.37 d (6.0)	41.3	3.58 d (5.5)	40.9	3.42 d (5.0)	41.8
2‴	5.58 t (6.0)	128.6	5.65 t (6.0)	129.6	5.73 t (6.0)	128.1	5.79 t (5.5)	127.4	5.74 t (5.0)	127.9
3‴	5.59 t (6.0)	130.2	5.65 t (6.0)	129.5	5.73 t (6.0)	130.9	5.79 t (5.5)	131.5	5.74 t (5.0)	131.2
4‴	3.98 t (6.0)	37.9	3.93 t (6.0)	42.2	3.96 t (6.0)	42.2	3.98 t (5.5)	42.2	3.97 t (5.0)	42.2
5‴		152.0		151.7		151.7		151.7		151.8
N′H	9.57 brs		9.61 brs		9.64 brs		9.64 brs		9.72 brs	
N‴H	9.62 brs		9.61 brs		9.64 brs		9.64 brs		9.64 brs	

[a]Data (δ) were measured in acetone-d_6 for **1**-**5** at 500 MHz for ^{1}H NMR and 125 MHz for ^{13}C NMR. Coupling constants (J) in Hz are given in parentheses. The assignments were based on DEPT, ^{1}H–^{1}H COSY, HSQC and HMBC experiments.

Table 2 NMR spectroscopic data for compounds **6** and **7**[a].

No.	**6** (DMSO-d_6)		**6** (Acetone-d_6)		**7** (MeOH-d_4)	
	δ_H	δ_C	δ_H	δ_C	δ_H	δ_C
2		176.7		177.6		177.2
3		48.4		49.5		
3a		128.9		130.3		
4a	7.04 brd (7.2)	124.3	7.07 dd (7.2, 0.6)	125.3	3.67 dd (10.2, 7.2)	50.0
4a					3.33 dd (10.2, 7.2)	
5	6.91 ddd (7.8, 7.2, 0.6)	122.0	6.91 ddd (7.8, 7.2, 0.6)	122.9	4.46 dt (7.8, 7.2)	50.5
6	7.27 ddd (7.8, 7.8, 0.6)	129.8	7.26 ddd (7.8, 7.2, 0.6)	130.5	5.94 ddd (17.4, 10.2, 7.8)	137.2
7a	6.93 brd (7.8)	110.1	7.01 brd (7.2)	110.9	5.26 d (17.4)	118.0
7b		142.7		143.7	5.10 d (10.2)	
3′		126.6		128.5		
4′	7.42 dd (5.4, 3.0)	141.3	7.42 dd (4.8, 4.2)	142.0		
5′a	2.79 m	26.6	2.83 m	27.8		
5′b	2.79 m		2.83 m			
6′a	3.56 ddd (15.6, 10.8, 4.8)	21.1	3.75 ddd (13.2, 8.4, 6.6)	22.2		
6′b	2.77 m		2.74 ddd (13.2, 4.2, 3.6)			
3″		173.0		174.2		
5″		185.4		187.2		
1‴a	2.81 dd (13.8, 7.2)	40.5	2.85 dd (14.4, 5.4)	41.4		
1‴b	2.75 dd (13.8, 6.6)		2.82 dd (14.4, 7.2)			
2‴	4.23 ddd (7.2, 6.6, 5.4)	70.0	4.37 dt (7.2, 5.4)	71.3		
3‴	5.63 ddd (16.8, 10.8, 5.4)	140.9	5.70 ddd (16.8, 10.8, 5.4)	141.5		
4‴a	5.02 dt (16.8, 1.8)	113.7	5.10 dt (16.8, 1.8)	114.1		
4‴b	4.89 dt (10.8, 1.8)		4.90 dt (10.8, 1.8)			
1-NH	10.74 s		9.69 s			
2‴-OH	4.83 d (5.4)		3.68 d (5.4)			

[a]Data (δ) were measured at 600 MHz for ^{1}H NMR and 150 MHz for ^{13}C NMR. Coupling constants (J) in Hz are given in parentheses. The assignments were based on DEPT, ^{1}H–^{1}H COSY, HSQC and HMBC experiments.

features of **3** resembled those of **2**. However, as compared the NMR spectroscopic data between **3** and **2** (Table 1), the chemical shifts of H_2-1′(H_2-1‴) and C-1′(C-1‴) in **3** were significantly deshielded by $\Delta\delta_H$ +0.26 and $\Delta\delta_C$ +9.0, respectively. This suggested replacement of the sulfide bond in **2** by a disulfide bond in **3**, which was verified by the 2D NMR data analysis (Figs. 2 and 3), particularly by the absence of the correlation from H_2-1′ to C-1‴ (H_2-1‴ to C-1′) in the HMBC spectrum of **3**. The presence of the disulfide bond was further proved by EI-MS data of **3** at *m/z* (%) 129 (100), 225 (7), and 256 (29) due to breakdown of the carbamide, carbon-sulfur, and disulfide bonds, respectively (Supplementary Information Fig. S51). The 5 *R*,5″*R*-configuration of **3** was supported by the specific rotation and CD data as well as by comparison of the experimental CD and calculated ECD spectra of **3** (Fig. 4). Therefore, the structure of compound **3** was determined and named isatithioetherin C.

Compound **4** was obtained as a colorless gum with $[\alpha]_D^{20}$ +28.0 (*c* 0.47, MeCN). The molecular formula of **4** was determined as $C_{20}H_{26}N_4O_4S_5$ with one more sulfur atom than that of **3** (Experimental Section 4.3 and Table 1). In addition, comparing the NMR spectroscopic data between the two compounds (Table 1), the chemical shifts of H_2-1′, H-2′, and H-3′ (H_2-1‴, H-2‴, and H-3‴) in **4** were changed by $\Delta\delta_H$ +0.21, +0.06, and +0.06 respectively. These differences revealed that **4** was the trisulfide derivative of **3**, which was also proved by 2D NMR data analysis of **4** (Figs. 2 and 3). Especially, the EI-MS data of **3** with successive losses of two sulfur atoms at *m/z* (%) 320 (6), 288 (23), and 256 (8) (Supplementary Information Fig. S66), further confirmed a liner linkage of the three sulfur atoms in **4**. Consistency of the specific rotation and CD data as well as the calculated ECD spectra of **4** and **3** (Figs. 4 and 5) indicated that stereochemistry of the two compounds was identical. Thus, the structure of compound **4** was determined and named isatithioetherin D.

Compound **5**, a colorless gum with $[\alpha]_D^{20}$ +39.2 (*c* 0.21, MeCN), is an isomer of **3** as indicated by spectroscopic data (Experimental Section 4.3 and Table 1). However, the NMR spectroscopic data showed that **5** had an asymmetric structure. Comparison of the NMR spectroscopic data between **5** and **3** (Table 1) demonstrated that a terminal double bond [δ_H 5.76 (1H, ddd, J = 17.0, 10.5, and 7.0 Hz, H-3′), 5.30 (1H, d, J = 17.0 Hz, H-4′a), and 5.23 (1H, d, J = 10.5 Hz, H-4′b); and δ_C 136.2 (C-3′) and 119.3 (C-4′)] and a sulfur-bearing methine [δ_H 3.68 (1 H, q, J = 7.0 Hz, H-2′) and δ_C 53.5 (C-2′)] in **5** replaced one *trans*-disubstituted double bond and one sulfur-bearing methylene in **3**. In addition, the resonances for one nitrogen-bearing methylene changed from δ_H 3.96 (2H, t, J = 6.0 Hz, H_2-4′) and δ_C 42.2 (C-4′) in **3** to δ_H 3.74 and 3.57 (1H each, dt J = 12.0 and 7.0 Hz, H-1′a and H-1′b) and δ_C 43.6 (C-1′) in **5**. This demonstrated replacement of the 4′-amino-but-2′-enyl unit in **3** by an 1′-amino-but-3′-en-2′-yl unit in **5**. The deduction was proved by the ^{1}H–^{1}H COSY cross peaks of N*H*/H_2-1′/H-2′/H-3′/H_2-4′, the HMBC correlations from H_2-1′ to C-5′, and the ROESY correlations between H_2-1‴ and H-3‴ and between H-2‴ and H_2-4‴ (Figs. 2 and 3). The chemical shifts of H_2-2′, H_2-2‴ and C-2′ and C-2‴, together with the molecular composition, demonstrated that a 1‴,2′-disulfide bond must be formed in **5**, which was further supported by EI-MS data (Supplementary Information Fig. S82). Similarity of the specific rotation and CD data between **5** and **3** suggested that they had the same 5 *R*,5″*R*-configuration.

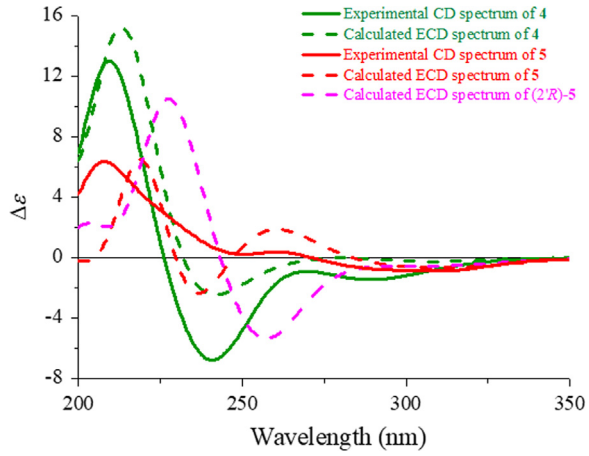

Figure 5 The overlaid experimental CD (full lines) and calculated ECD spectra (dash lines) of compounds **4**, **5**, and (2′*R*)-**5**.

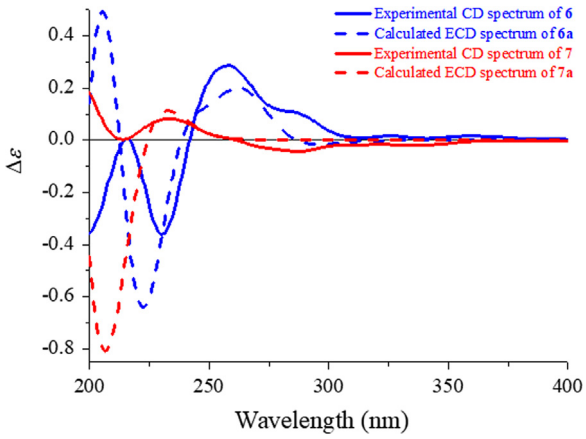

Figure 6 The experimental CD spectra of **6** (10 times reduced) and **7** (full lines) overlaid with the calculated ECD spectra of compounds **6a** (10 times reduced) and **7a** (dash lines).

Especially, the experimental CD spectrum of **5** matched well with the calculated ECD spectrum (Fig. 5), but significantly differed from that of the 2′-epimer of **5** (Supplementary Information Figs. S10 and S12). This supported that **5** had the 2′*S*,5*R*″*R*-configuration. Therefore, the structure of compound **5** was determined and named isatithioetherin E.

Compound **6** was obtained as a colorless gum with $[\alpha]_D^{20}$ +15.2 (*c* 0.24, MeOH). Its spectroscopic data were similar to those of the scalemic mixture of **9a** and **9b** in a 2:1 ratio from the same decoction[49] [herein, given trivial names (−)-isatithiopyrin A for **9a** and (+)-isatithiopyrin A for **9b**, respectively]. However, TLC and reversed-phase HPLC analysis indicated that **6** was different from **9**. Comparison of the NMR spectroscopic data between **6** (Table 2) and **9** in the same solvent DMSO-d_6[49] demonstrated that H-1‴a and 2‴-O*H* in **6** were shielded by $\Delta\delta_H$ −0.05 and −0.10, respectively, whereas H-1‴b, H-2‴, H-3‴, H-4‴a, and H-4‴b were deshielded by $\Delta\delta_H$ +0.05, +0.06, +0.16, +0.23, and +0.12, while differences of the chemical shifts for the other proton resonances and all the carbon resonances were less than $\Delta\delta_H$ ±0.03 and $\Delta\delta_C$ ±0.3. Based on these changes and the optical activity, **6** was deduced as either a diastereomer of **9a** and **9b** or a scalemic mixture of the diastereomers of **9a** and **9b**, which was further confirmed by 2D NMR data analysis of **6** in both the solvents of acetone-d_6 and DMSO-d_6 (Fig. 2). Because the specific rotation data of **6** was opposite to that of **9** with almost an equal magnitude and because the later was proved as the scalemic mixture of **9a** and **9b** in a 2:1 ratio[49], **6** must be a mixture containing two enantiomers in the same 2:1 ratio. Although subsequent chiral HPLC separation proved the presence of two partially resolved peaks with an integration of about 2:1 ratio in the chromatogram of **6** (Supplementary Information Figs. S113 and S114), further isolation of the two components failed due to decomposition of the sample in solid state storing at 10 °C for 6 months. Since two chiral centers exist in the structures, there are only four stereoisomers including two pairs of enantiomers. With the previous chiral separation and structural assignment of **9a** and **9b** as the (−)-(2‴*S*,3*S*)- and (+)-(2‴*R*,3*R*)-enantiomers[49,62], respectively, **6** must be a mixture consisting of (2‴*S*,3*R*)- and (2‴*R*,3 *S*)-enantiomers in the approximate 2:1 or 1:2 ratio and the optical properties of **6** must be from the exceed enantiomer. The experimental spectrum of **6** was in good agreement with the theoretically calculated ECD spectrum of the (2‴*S*,3*R*)-enantiomer (**6a**, Fig. 6), whereas mirrored to that of the (2‴*R*,3*S*)-enantiomer (**6b**) (Supplementary Information Fig. S14). This supported that **6** consisted of **6a** and **6b** in the approximate 2:1 ratio and that the positive specific rotation of **6** was from the exceed **6a**. Accordingly, **6b** must has the negative specific rotation. Therefore, the structures of compounds **6a** and **6b** were assigned and named as (+)-and (−)-isatithiopyrin B, respectively. It is worth noting that the four stereoisomers were very recently synthesized by a biomimetic thio-Diels–Alder reaction, a very rare reaction in nature, and that the presence of **6a** and **6b** in the 2:1 ratio was also predicted by density functional theory (DFT) calculations[62]. Therefore, compounds **6a** and **6b** are new natural products, which were chemically synthesized and theoretically predicted.

Compound **7** was obtained as a colorless gum with $[\alpha]_D^{20}$ +26.3 (*c* 0.1, MeOH). Its spectroscopic features was similar to those of **8** (the scalemic mixture of **8a** and **8b** in the 2:1 ratio[64]), indicating that **7** was either an isomer of **8a** and **8b** or a scalemic mixture of the isomers of **8a** and **8b**. As compared with those of **8**, the H-5 and C-5 resonances in the NMR spectra of **7** were significantly shielded by $\Delta\delta_H$ −0.90 and $\Delta\delta_C$ −30.0, respectively, while the C-2 resonance was shielded by $\Delta\delta_C$ −10.0. The differences indicated isomerization of the oxazolidine-2-thione ring in **8** into a thiazolidin-2-one ring in **7,** which was proved by 2D NMR data analysis of **7** (Fig. 2). HPLC analysis using a chiral column (CD-ph) confirmed that **7** was a scalemic mixture of the enantiomers **7a** and **7b** in the 2:1 ratio (Supplementary Information Fig. S126). Although further preparative separation of the enantiomers failed due to decomposition of the sample in solid state during storage, similarity of the specific rotation and CD curve between **7** with **8** and **8a** indicated that the exceed enantiomer in **7** had the same configuration as **8a**. This was further supported by comparing the experimental CD spectrum of **7** with the theoretically calculated spectra of **7a** and **7b** (Fig. 6). Therefore, the structure of **7a** and **7b** were determined and named as isoepigoitrin and isogoitrin, respectively.

Compounds **1**−**5** are the first example of natural products with dimeric structure features likely deriving from epigoitrin (**8a**). Based on our previous speculations, these sulfur-containing metabolites are biosynthesized (Scheme 1) from the precursors glucosinolates[49,55] including epiprogoitrin (**10**) and/or progoitrin (**11**) also, which are abundant in the 2:1 ratio of **10**:**11** in *I. indigotica*[64]. Myrosinases catalyzed hydrolysis of epiprogoitrin (**10**) and progoitrin (**11**)

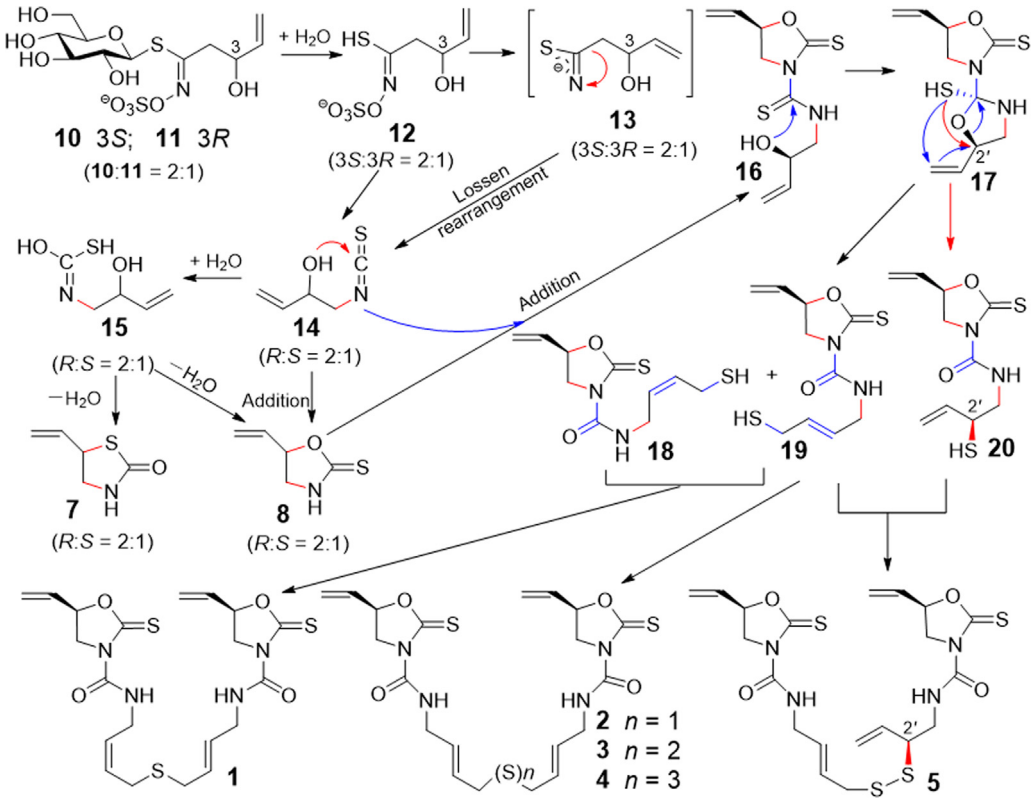

Scheme 1 Proposed biosynthetic pathways of compounds **1**–**5**, **7**, and **8**.

liberates intermediate **12**, which undergoes the Lossen rearrangement, either *via* a direct process or *via* imidothioate **13**, to yield isothiocyanate **14**. An intermolecular nucleophilic addition of **14** produces **8**[65]. Isolation of **7** indicates the possible presence of enzyme-catalyzed hydrolysis and dehydration processes of **14** *via* an unstable intermediate **15** to generate both **7** and **8**, because the proportion and configuration of the exceed enantiomers in the scalemic mixtures are sustained. In a stereoselective manner, an enzyme-catalyzed nucleophilic intermolecular addition between the *R*-isomers of **8** and **14** would give the optically active intermediate **16**. A further intramolecular addition of **16** generates an intermediate **17**, which undergoes migration of the thiol group to the terminal double-bond with simultaneous double bond rearrangement and breakdown of the oxygen-bridge to afford the thiol carbamides **18** and **19** (geometric isomers). The thiol group in **17** would also be migrated to the oxygen-bridged methine carbon to afford the thiol carbamide **20**, accompanying with reversion of the C-2′ configuration from 2′*R* in **17** to 2′*S* in **20**. Condensation between **18** and **19** and between two molecules of **19** produces **1** and **2**, respectively. Meanwhile, a molecule of H_2S would be simultaneously liberated as a sulfur donor to form the disulfide **3** and trisulfide **4** from **19** as well as to form disulfide **5** from **19** and **20**. Moreover, together with **9a** and **9b**[49], the isolation and structure determination of **6a** and **6b** confirmed biosynthetic formation of the stereoisomers *via* a rare thio-Diels–Alder reaction in nature[62]. The experimental data demonstrate that the configuration at the spiro carbon (C-3) plays a decisive role in the specific rotations and the CD spectroscopic features of **6a**, **6b**, **9a**, and **9b**. The biogenetic speculations fully support the structural assignments of **1**–**9**.

Although the postulated biosynthetic precursors occur as the stereoisomers epiprogoitrin (**10**) and progoitrin (**11**) in the inequivalent amounts (2:1), **1**–**5** were obtained as the optically pure forms and their diastereomers were not founded in the decoction. The fact indicates that **1**–**5** are biosynthesized in a stereoselective manner, implying the presence of specific enzyme(s) to control the stereoselectivity. Additionally, the precursors glucosinolates can thermally be decomposed into diverse bioactive breakdown products[65]. Therefore, influences of the decocting process on the bioactive components as well as the pharmacological effects of the ban lan gen decoction deserves further investigation in future studies.

In the preliminary *in vitro* assays, compounds **2** and **4** showed antiviral activity against influenza virus A/Hanfang/359/95 (H3N2)[66], with IC_{50} values of 0.60 and 1.92 μmol/L and SI values of 9.62 and 3.61, respectively (the positive control RBV, IC_{50} = 0.97 μmol/L and SI = 1200). These two compounds also exhibited activity against the herpes simplex virus 1 (HSV-1)[66] with IC_{50} values of 3.70 and 2.87 μmol/L and SI values of 5.20 and 2.68, respectively (the positive control acyclovir, IC_{50} = 0.71 μmol/L and SI = 140.9). In addition, **2** inhibited Coxsackie virus B3 replication[66], with IC_{50} and SI values of 0.71 μmol/L and 9.04 (the positive control Pleconaril, IC_{50} = 0.41 μmol/L and SI = 243.9; RBV, IC_{50} = 222.22 μmol/L and SI = 9.0). Moreover, **2** and **4** reduced D,L-galactosamine (GAlN)-induced hepatocyte (WB-F344 cell) damage[67] with 70% and 73% inhibition at 10 μmol/L, respectively, while the positive control bicyclol gave 66% inhibition.

3. Conclusions

From the aqueous extract of the *I. indigotica* root, five novel sulfur-enriched alkaloids isatithioetherins A − E (**1** − **5**), together

with two pairs of scalemic enantiomers (+)- and (−)-isatithiopyrin B (**6a** and **6b**) and isoepigoitrin and isogoitrin (**7a** and **7b**) were isolated and structurally determined. Compounds **1**–**5** represent the first examples of sulfur-enriched natural products biogenetically assembled by four epigoitrin-derived units, while **6a** and **6b** having the unique structural feature are the scalemic mixture (2:1), which were biomimetically synthesized by the rare thio-Diels–Alder reaction and theoretically predicted by the DFT calculations[62]. The relatively broad antiviral spectra of **2** and **4** demonstrate that the sulfur-enriched metabolites are potentially active constituents responsible for the treatment of influenza and other diseases in clinic application of the ban lan gen decoction, though other compounds were not assayed due to limitation of the sample amounts and/or decomposition of the compounds during storage. The labile properties of the novel sulfur-enriched compounds indicate that the decocting procedure must be an important factor to significantly influence on content and composition of the chemical constituents in the ban lan gen extracts. Therefore, the extracting process must be taken into consideration in research and evaluation of ban lan gen and da qing ye. This consideration would also be valid for some of the other herbal medicines. Additionally, our previous and present results[48–61] reveal that, in the ban lan gen decoction there are diverse active components against different types of viruses and continuously provide novel candidate for further studies of synthetic/biosynthetic and medicinal chemistry as well as pharmacology.

4. Experimental

4.1. General experimental procedures

Optical rotations were measured on a P-2000 polarimeter (JASCO, Tokyo, Japan). UV spectra were acquired on a V-650 spectrometer (JASCO, Tokyo, Japan). CD spectra were measured on a JASCO J-815 CD spectrometer (JASCO, Tokyo, Japan). IR spectra were obtained on a Nicolet 5700 FT-IR microscope instrument (FT-IR microscope transmission, Thermo Electron Corporation, Madison, WI, USA). NMR spectra were recorded at 600 or 500 MHz for ^{1}H NMR and 150 or 125 MHz for ^{13}C NMR, respectively, on a SYS 600 instrument (Varian Associates Inc., Palo Alto, CA, USA) or Bruker 500 NMR (Bruker Corp. Karlsruhe, Germany) spectrometer in DMSO-d_6, acetone-d_6 or MeOH-d_4 with TMS or solvent peaks used as references. EI-MS data were measured on an AutoSpec Ultima-TOF spectrometer (Micromass, UK). ESI-MS and HR-ESI-MS data were taken on an Agilent 1100 Series LC-MSD-Trap-SL and an Agilent 6520 Accurate-Mass Q-TOF LCMS spectrometers (Agilent Technologies, Ltd., Santa Clara, CA, USA), respectively. Column chromatography (CC) was carried out on macroporous adsorbent resin (HPD-110, Cangzhou Bon Absorber Technology Co., Ltd., Cangzhou, China), CHP 20 P (Mitsubishi Chemical Inc., Tokyo, Japan), silica gel (200–300 mesh, Qingdao Marine Chemical Inc., Qingdao, China), Sephadex LH-20 (Pharmacia Biotech AB, Uppsala, Sweden), or reversed phase C-18 silica gel (W. R. Grace & Co., Maryland, USA). HPLC separation was performed on an instrument equipped with an Agilent ChemStation for LC system, an Agilent 1200 pump, and an Agilent 1100 single-wavelength absorbance detector (Agilent Technologies, Ltd.) using a Grace semipreparative column (250 mm × 10 mm i.d.) packed with C18 reversed phase silica gel (5 μm) (W. R. Grace & Co., Maryland, USA), an analytical CD-Ph column (250 mm × 4.6 mm, Shiseido China Co., Ltd., Shanghai, China) column, or a semipreparative Chiralpak AD-H or Chiralpak IC column (250 mm × 10 mm, Daicel Chiral Technologies Co.). TLC was carried out on glass precoated silica gel GF_{254} plates (Qingdao Marine Chemical Inc.). Spots were visualized under UV light or by spraying with 7% H_2SO_4 in 95% EtOH followed by heating. Unless otherwise noted, all chemicals were purchased from commercially available sources and were used without further purification.

4.2. Plant material

The *I. indigotica* roots (ban lan gen) were collected in December 2009 from Bozhou, Anhui Province, China. Plant identity was verified by Mr. Lin Ma (Institute of Materia Medica, Beijing, China). A voucher specimen (No. ID-S-2385) was deposited at the herbarium of Natural Medicinal Chemistry, Institute of Materia Medica.

4.3. Extraction and isolation

The air-dried and pulvarized plant material (50 kg) was decocated with H_2O (150 L, 3 × 1 h). The aqueous extracts were combined and evaporated under reduced pressure to yield a dark-brown residue (32 kg). The residue was dissolved in H_2O (122L), loaded on a macroporous adsorbent resin (HPD-110, 19 kg) column (200 cm × 20 cm), and eluted successively with H_2O (50 L), 50% EtOH (125 L), and 95% EtOH (100 L) to yield three corresponding fractions A, B and C. After removing the solvent under reduced pressure, fraction B (0.9 kg) was separated by column chromatography (CC) over MCI gel CHP 20P (5 L), with successive elution using H_2O (10 L), 30% EtOH (30 L), 50% EtOH (20 L), 95% EtOH (10 L), and Me_2CO (8 L), to give fractions B1–B5. Fraction B2 (547 g) was subjected to CC over silica gel, with elution by a gradient of increasing MeOH concentration (0–100%) in EtOAc and then with 30% EtOH, to yield fractions B2-1–B2-5 based on TLC analysis. Fraction B2-1 (16.3 g) was chromatographed over Sephadex LH-20 with elution by a petroleum ether/chloroform/methanol (5:5:1) mixture to yield B2-1-1–B2-1-10. Fraction B2-1-1 (2.5 g) was separated by silica gel CC ($CHCl_3$/Me_2CO, 100:1) to give B2-1-1-1–B2-1-1-6. Subsequent separation of B2-1-1-3 (54.3 mg) by reversed-phase (RP) HPLC (63% CH_3CN in H_2O) gave **4** (15.2 mg) and **5** (2.3 mg). Fraction B2-1-1-4 (120.1 mg) was chromatographed over Sephadex LH-20 ($CHCl_3$/MeOH, 1:1) to give fractions B2-1-1-4-1 and B2-1-1-4-2, of which B2-1-1-4-1 (34.2 mg) was purified by preparative TLC (mobile phase: $CHCl_3$/Me_2CO, 15:1) to yield **1** (2.6 mg), and B2-1-1-4-2 by RP HPLC (63% CH_3CN in H_2O) to afford **2** (18.7 mg). Fraction B2-1-1-6 (122.7 mg) was separated by RP flash CC (0–100% MeOH in H_2O) to give **3** (8.2 mg). B2-1-2 (600 mg) was fractionated by RP flash CC with a gradient of increasing MeOH concentration (0–100%) in H_2O to yield B2-1-2-1–B2-1-2-4. Separation of B2-1-2-4 (10.7 mg) by RP HPLC (60% MeOH in H_2O) afforded **6** (1.9 mg) and **9** (2.1 mg). Chiral HPLC analysis of **6** using AD-H column (250 mm × 10 mm) and mobile phase iPrOH–*n*-hexane (1:4, 2.0 mL/min) showed two peaks (**6a** and **6b**) with an approximate integration ratio of 2:1. B2-1-3 (7.6 g) was fractioned by silica gel CC ($CHCl_3$/MeOH, 50:1) to give B2-1-3-1 − B2-1-3-3, of which B2-1-3-1 (5 g) was chromatographed over silica gel CC (petroleum ether/Me_2CO, 10:1) to yield **8** (3.5 g). Subsequent separation of **8** (20 mg) by HPLC using Chiralpak IC column (250 mm × 10 mm) and mobile phase

iPrOH–*n*-hexane mixture (1:6, 2 mL/min) yielded **8a** (12.2 mg) and **8b** (6.1 mg). B2-1-3-2 (30.5 mg) was isolated by RP HPLC (27% MeOH in H_2O) to obtain **7** (2.5 mg). Chiral HPLC analysis of **7** using CD-ph column (250 mm × 4.6 mm) and gradient elution increasing MeCN in H_2O (20:80–65:35 in 12.0 min, 1.5 mL/min) showed two peaks (**7a** and **7b**) with an approximate integration ratio of 2:1.

4.3.1. *Isatithioetherin A (**1**)*

Colorless gum; $[\alpha]_D^{20}$ +38.8 (*c* 0.1, MeCN); UV (MeOH) λ_{max} (logε) 258 (4.53) nm; CD (MeCN) 204 ($\Delta\varepsilon$+2.90), 242 ($\Delta\varepsilon$+0.29), 273 ($\Delta\varepsilon$ −0.24), 301 ($\Delta\varepsilon$ −0.54) nm; IR ν_{max} 3338, 3208, 3040, 2919, 1702, 1542, 1477, 1403, 1350, 1233, 1200, 1094, 1047, 966, 859, 803, 753, 721, 651, 595 cm^{-1}; ^1H NMR (acetone-d_6, 500 MHz) data Table 1; ^{13}C NMR (acetone-d_6, 125 MHz) data Table 1; (+)-ESI-MS *m/z* 505 $[M + Na]^+$, 521 $[M + K]^+$; (−)-ESI-MS *m/z* 517 $[M+Cl]^-$; (+)-HR-ESI-MS *m/z* 483.1206 $[M+H]^+$ (Calcd. for $C_{20}H_{27}N_4O_4S_3$, 483.1189), 505.1017 $[M+Na]^+$ (Calcd. for $C_{20}H_{26}N_4O_4S_3Na$, 505.1008).

4.3.2. *Isatithioetherin B (**2**)*

Colorless gum; $[\alpha]_D^{20}$ +32.0 (*c* 1.7, MeCN); UV (MeOH) λ_{max} (logε) 257 (4.50) nm; CD (MeCN) 216 ($\Delta\varepsilon$ +4.02), 254 ($\Delta\varepsilon$ +0.34), 293 ($\Delta\varepsilon$ −0.75), 309 ($\Delta\varepsilon$ −0.81) nm; IR ν_{max} 3210, 3042, 2916, 1703, 1541, 1477, 1403, 1350, 1233, 1196, 1094, 1045, 967, 858, 810, 753, 651, 594 cm^{-1}; ^1H NMR (acetone-d_6, 500 MHz) data Table 1; ^{13}C NMR (acetone-d_6, 125 MHz) data Table 1; EI-MS *m/z* (%) 225 (22), 149 (13), 129 (100), 95 (63), 85 (45), 68 (61); (+)-ESI-MS *m/z* 505 $[M + Na]^+$, 521 $[M + K]^+$; (−)-ESI-MS *m/z* 517 $[M + Cl]^-$; (+)-HR-ESI-MS *m/z* 483.1204 $[M + H]^+$ (Calcd. for $C_{20}H_{27}N_4O_4S_3$, 483.1189), 505.1019 $[M + Na]^+$ (Calcd. for $C_{20}H_{26}N_4O_4S_3Na$, 505.1008).

4.3.3. *Isatithioetherin C (**3**)*

Colorless gum; $[\alpha]_D^{20}$ +30.4 (*c* 0.2, MeCN); UV (MeOH) λ_{max} (logε) 257 (4.48) nm; CD (MeCN) 215 ($\Delta\varepsilon$ +1.28), 305 ($\Delta\varepsilon$ −0.49) nm; IR ν_{max} 3336, 3211, 3032, 2922, 1702, 1541, 1477, 1403, 1352, 1233, 1196, 1044, 950, 858, 753, 651, 590 cm^{-1}; ^1H NMR (acetone-d_6, 500 MHz) data Table 1; and ^{13}C NMR (acetone-d_6, 125 MHz) data Table 1; EI-MS *m/z* (%) 256 (29), 225 (7), 149 (25), 129 (100), 118 (32), 96 (62), 85 (29), 69 (87); (+)-ESI-MS *m/z* 515 $[M + H]^+$, 537 $[M + Na]^+$; (−)-ESI-MS *m/z* 549 $[M + Cl]^-$; (+)-HR-ESI-MS *m/z* 515.0918 $[M + H]^+$ (Calcd. for $C_{20}H_{27}N_4O_4S_4$, 515.0910), 537.0736 $[M + Na]^+$ (Calcd. for $C_{20}H_{26}N_4O_4S_4Na$, 537.0729).

4.3.4. *Isatithioetherin D (**4**)*

Colorless gum; $[\alpha]_D^{20}$ +28.0 (*c* 0.47, MeCN); UV (MeOH) λ_{max} (logε) 258 (4.40) nm; CD (MeCN) 218 ($\Delta\varepsilon$ +3.53), 255 ($\Delta\varepsilon$ +0.24), 291 ($\Delta\varepsilon$ −0.80), 312 ($\Delta\varepsilon$ −0.79) nm; IR ν_{max} 3207, 3040, 2917, 1702, 1540, 1477, 1403, 1349, 1232, 1196, 1168, 1094, 1046, 965, 859, 812, 752, 650, 594 cm^{-1}; ^1H NMR (acetone-d_6, 500 MHz) data Table 1; ^{13}C NMR (acetone-d_6, 125 MHz) data Table 1; EI-MS *m/z* (%) 320 (6), 288 (23), 256 (8), 225 (12), 129 (100), 118 (11), 96 (23), 85 (32), 68 (52); (+)-ESI-MS *m/z* 569 $[M+Na]^+$; (+)-HR-ESI-MS *m/z* 547.0639 $[M+H]^+$ (Calcd. for $C_{20}H_{27}N_4O_4S_5$, 547.0630), 569.0452 $[M+Na]^+$ (Calcd. for $C_{20}H_{26}N_4O_4S_5Na$, 569.0450).

4.3.5. *Isatithioetherin E (**5**)*

Colorless gum; $[\alpha]_D^{20}$ +39.2 (*c* 0.21, MeCN); UV (MeOH) λ_{max} (logε) 258 (4.56) nm; CD (MeCN) 208 ($\Delta\varepsilon$ +6.37), 261 ($\Delta\varepsilon$ +0.38), 292 ($\Delta\varepsilon$ −0.78), 314 ($\Delta\varepsilon$ −0.83) nm; IR ν_{max} 3204, 3050, 2921, 2855, 1702, 1541, 1477, 1402, 1350, 1232, 1196, 1095, 1046, 965, 948, 859, 808, 753, 651, 593 cm^{-1}; ^1H NMR (acetone-d_6, 500 MHz) data Table 1; ^{13}C NMR (acetone-d_6, 125 MHz) data Table 1; EI-MS *m/z* (%) 320 (3), 288 (18), 256 (6), 223 (5), 129 (100), 118 (12), 96 (26), 85 (34), 68 (54); (+)-ESI-MS *m/z* 537 $[M + Na]^+$, 553 $[M + K]^+$; (−)-ESI-MS *m/z* 549 $[M + Cl]^-$; (+)-HR-ESI-MS *m/z* 515.0916 $[M + H]^+$ (Calcd. for $C_{20}H_{27}N_4O_4S_4$, 515.0910); 537.0732 $[M + Na]^+$ (Calcd. for $C_{20}H_{26}N_4O_4S_4Na$, 537.0729).

4.3.6. *(+)- and (−)-isatithiopyrin B (**6a** and **6b**) in a 2:1 ratio*

Colorless gum; $[\alpha]_D^{20}$ +15.2 (*c* 0.24, MeOH); UV (MeOH) λ_{max} (logε) 209 (4.37), 250 (sh, 3.56) nm; CD (MeCN) 231 ($\Delta\varepsilon$ −3.61), 259 ($\Delta\varepsilon$ +2.87), 284 ($\Delta\varepsilon$ +1.10) nm; IR ν_{max} 3255, 3089, 3026, 2924, 2852, 1716, 1619, 1474, 1413, 1321, 1243, 1184, 1135, 1107, 1077, 1027, 997, 929, 835, 753, 721, 690, 633, 564, 492 cm^{-1}; ^1H NMR (acetone-d_6, 600 MHz) data Table 2, ^1H NMR (DMSO-d_6, 600 MHz) data Table 2, ^{13}C NMR (acetone-d_6, 150 MHz) data Table 2, ^{13}C NMR (DMSO-d_6, 150 MHz) data Table 2; (+)-ESI-MS *m/z* 372 $[M + H]^+$, 394 $[M + Na]^+$, 410 $[M + K]^+$; (−)-ESI-MS *m/z* 406 $[M + Cl]^-$; (+)-HR-ESI-MS *m/z* 372.0849 $[M + H]^+$ (Calcd. 372.0835 for $C_{18}H_{18}N_3O_2S_2$), 394.0667 $[M + Na]^+$ (Calcd. 394.0654 for $C_{18}H_{17}N_3O_2S_2Na$).

4.3.7. *Isoepigoitrin and Isogoitrin (**7a** and **7b**) in a 2:1 ratio*

Colorless gum; $[\alpha]_D^{20}$ +26.3 (*c* 0.1, MeOH); UV (MeOH) λ_{max} (logε) 207 (4.12), 250 (sh, 1.22) nm; CD (MeCN) 233 ($\Delta\varepsilon$ +0.08), 287 ($\Delta\varepsilon$ −0.04), 339 ($\Delta\varepsilon$ −0.02) nm; IR (KBr) ν_{max} 3245, 3087, 2982, 2879, 1679, 1539, 1473, 1420, 1355, 1296, 1245, 1214, 1138, 1070, 989, 969, 930, 799, 723, 677, 614 cm^{-1}; ^1H NMR (MeOH-d_4, 600 MHz) data Table 2; ^{13}C NMR (MeOH-d_4, 150 MHz) data Table 2; EI-MS *m/z* (%) 129 $[M]^{\cdot +}$ (63), 96 (27), 85 (64), 73 (100), 71 (61), 69 (90), 57 (40); (+)-HR-ESI-MS *m/z* 130.0320 $[M+H]^+$ (Calcd. for C_5H_8NOS, 130.0321), 152.0136 $[M+H]^+$ (Calcd. for C_5H_8NOSNa, 152.0141).

4.3.8. *ECD calculations of **1**–**5**, **6a/6b**, and **7a/7b***

For details, see Supplementary Information. Briefly, conformational analysis and quantum computations were performed using Gaussian 16 program package. The lowest energy conformers whose relative energy within 4 kcal/mol were further optimized at the B3LYP/6–31 g(d,p) level. The energies, oscillator strengths, and rotational strengths were calculated using the TDDFT methodology at the CAM-B3LYP/6–311+G (d,p) level. Conductor-like polarizable continuum model (CPCM) was adopted to consider solvent effects using the dielectric constant of MeCN (ε = 35.7) for **1**–**5** and **7** and MeOH (ε = 32.6) for **6**.

Acknowledgments

Financial support from the National Natural Sciences Foundation of China (NNSFC; Grant Nos. 81373287, 81630094, 81730093, and 21732008), and CAMS Innovation Fund for Medical Sciences (Grant Nos. 2017-I2M-3-010, 2016-I2M-1-010, and 2016-I2M-1-004) are acknowledged and Non-profit Central Research Institute

Fund of Chinese Academy of Medical Sciences (Grant Nos. 2018PT35002 and 2017PT35001).

Appendix A. Supporting information

Supplementary data associated with this article can be found in the online version at https://doi.org/10.1016/j.apsb.2018.08.005.

References

1. Jiangsu New Medical College. *Dictionary of traditional Chinese medicine*, 1. Shanghai: Shanghai Scientific and Technical Publishers; 1986. p.126, 1250.
2. Lin AH, Fang SX, Fang JG, Du G, Liu YH. Studies on anti-endotoxin activity of F_{022} from *Radix Isatidis*. *China J Chin Mater Med* 2002;**27**:439–42.
3. Wu X, Qin G, Cheung KK, Cheng KF. New alkaloids from *Isatis indigotica*. *Tetrahedron* 1997;**53**:13323–8.
4. Wu X, Liu Y, Sheng W, Sun J, Qin G. Chemical constituents of *Isatis indigotica*. *Planta Med* 1997;**63**:55–7.
5. Li B, Chen WS, Zheng SQ, Yang GJ, Qiao CZ. Two new alkaloids isolated from tetraploidy banlangen. *Acta Pharm Sin* 2000;**35**:508–10.
6. Chen WS, Li B, Zhang WD, Yang GJ, Qiao CZ. A new alkaloid from the root of *Isatis indigotica* Fort. *Chin Chem Lett* 2001;**12**:501–2.
7. Wei XY, Leung CY, Wong CK, Shen XL, Wong RN, Cai ZW, et al. Bisindigotin, a TCDD antagonist from the Chinese medicinal herb *Isatis indigotica*. *J Nat Prod* 2005;**68**:427–9.
8. Liu JF, Jiang ZY, Wang RR, Zheng YT, Chen JJ, Zhang XM, et al. Isatisine A, a novel alkaloid with an unprecedented skeleton from leaves of *Isatis indigotica*. *Org Lett* 2007;**9**:4127–9.
9. Sun DD, Dong WW, Li X, Zhang HQ. Indole alkaloids from the roots of *Isatis ingigotica* and their antiherpes simplex virus type 2 (HSV-2) activity *in vitro*. *Chem Nat Comp* 2010;**46**:763–6.
10. Wu Y, Zhang ZX, Hu H, Li D, Qiu G, Hu X, et al. Novel indole C-glycosides from *Isatis indigotica* and their potential cytotoxic activity. *Fitoterapia* 2011;**82**:288–92.
11. Li B, Chen WS, Zhao Y, Zhang HM, Dong JX, Qiao CZ. Phenylpropanoids isolated from tetraploid roots of *Isatis indigotica*. *Chin Tradit Herb Drugs* 2005;**36**:326–8.
12. Xie Z, Shi Y, Wang Z, Wang R, Li Y. Biotransformation of glucosinolates epiprogoitrin and progoitrin to (*R*)- and (*S*)-goitrin in *Radix isatidis*. *J Agric Food Chem* 2011;**59**:12467–72.
13. Zuo L, Li JB, Xu J, Yang JZ, Zhang DM, Tong YL. Studies on chemical constituents in root of *Isatis indigotica*. *China J Chin Mater Med* 2007;**32**:688–91.
14. Sun DD, Dong WW, Li X, Zhang HQ. Isolation, structural determination and cytotoxic activity of two new ceramides from the root of *Isatis indigotica*. *Sci China Ser B: Chem* 2009;**52**:621–5.
15. He Y, Lu J, Lin RC. Studies on chemical constituents in root of *Isatis indigotica*. *Chin Tradit Herb Drugs* 2003;**34**:777–8.
16. Liu JF, Zhang XM, Xue DQ, Jiang ZY, Gu Q, Chen JJ. Studies on chemical constituents from leaves of *Isatis indigotica*. *China J Chin Mater Med* 2006;**31**:1961–5.
17. Huang QS, Yoshihira K, Natori S. Isolation of 2-hydroxy-3-butenyl thiocyanate, epigoitrin, and adenosine from 'banlangen', *Isatis indigotica* Root. *Planta Med* 1981;**42**:308–10.
18. He LW, Li X, Chen JW, Sun DD, Ju WZ, Wang KC. Chemical constituents from water extract of *Radix isatidis*. *Acta Pharm Sin* 2006;**41**:1193–6.
19. Bai J, Xiao H, He JW, Yan YX, Wang YS, Yang SL. Chemical constituents of *Radix Isatis*. *China J Chin Mater Med* 2007;**32**:271–2.
20. Liu R, Yuan B, Liu Z, Li X, Xiong Z, Li F. Identification of 5 constituents of the aqueous extract of *Isatis indigotica* by HPLC–MS^2. *J Chin Med Mater* 2005;**9**:772–4.
21. He L, Li X, Chen J, Wu J, Sun D. Studies on water-soluble chemical constitutions in *Radix Isatidis*. *China Pharm* 2006;**17**:232–4.
22. Liu HL, Wu LJ, Li H, Wang J. Study on the chemical constituents of *Isatis indigotica* Fort. *J Shenyang Pharm Univ* 2002;**19**:93–105 100 .
23. He LW, Dong W, Yang JY, Li X, Li W. Chemical constituents in antiviral fraction of *Isatidis Radix* and their activities. *Chin Tradit Herbal Drugs* 2013;**44**:2960–4.
24. Yang ZF, Wang YT, Qin S, Zhao SS, Zhao YS, Lin Q, et al. The effects of a hot water soluble extract (S-03) isolated from *Isatis indigotica* root on influenza A and B viruses *in vitro*. *Chin J Virol* 2011;**27**:218–23.
25. Xu WD, Tian Y, Guo QL, Yang YC, Shi JG. Secoeuphoractin, a minor diterpenoid with a new skeleton from *Euphorbia micractina*. *Chin Chem Lett* 2014;**25**:1531–4.
26. Tian Y, Guo Q, Xu W, Zhu C, Yang Y, Shi J. A minor diterpenoid with a new 6/5/7/3 fused-ring skeleton from *Euphorbia micractina*. *Org Lett* 2014;**16**:3950–3.
27. Song WX, Yang YC, Shi JG. Two new β-hydroxy amino acid-coupled secoiridoids from the flower buds of *Lonicera japonica*: isolation, structure elucidation, semisynthesis, and biological activities. *Chin Chem Lett* 2014;**25**:1215–9.
28. Jiang ZB, Song WX, Shi JG. Two 1-(6′-*O*-acyl-β-D-glucopyranosyl) pyridinium-3-carboxylates from the flower buds of *Lonicera japonica*. *Chin Chem Lett* 2015;**26**:69–72.
29. Yu Y, Jiang Z, Song W, Yang Y, Li Y, Jiang J, et al. Glucosylated caffeoylquinic acid derivatives from the flower buds of *Lonicera japonica*. *Acta Pharm Sin B* 2015;**5**:210–4.
30. Song WX, Guo QL, Yang YC, Shi JG. Two homosecoiridoids from the flower buds of *Lonicera japonica*. *Chin Chem Lett* 2015;**26**:517–21.
31. Jiang Y, Liu Y, Guo Q, Jiang Z, Xu C, Zhu C, et al. Acetylenes and fatty acids from *Codonopsis pilosula*. *Acta Pharm Sin B* 2015;**5**:215–22.
32. Jiang YP, Liu YF, Guo QL, Jiang ZB, Xu CB, Zhu CG, et al. C_{14}-Polyacetylene glucosides from *Codonopsis pilosula*. *J Asian Nat Prod Res* 2015;**17**:601–14.
33. Jiang YP, Liu YF, Guo QL, Shi JG. C_{14}-Polyacetylenol glycosides from the roots of *Codonopsis pilosula*. *J Asian Nat Prod Res* 2015;**17**:1166–79.
34. Jiang YP, Guo QL, Liu YF, Shi JG. Codonopiloneolignanin A, a polycyclic neolignan with a new carbon skeleton from the roots of *Codonopsis pilosula*. *Chin Chem Lett* 2016;**27**:55–8.
35. Jiang Y, Liu Y, Guo Q, Xu C, Zhu C, Shi J. Sesquiterpene glycosides from the roots of *Codonopsis pilosula*. *Acta Pharm Sin B* 2016;**6**:46–54.
36. Jiang ZB, Jiang BY, Zhu CG, Guo QL, Peng Y, Wang XL, et al. Aromatic acid derivatives from the lateral roots of *Aconitum carmichaelii*. *J Asian Nat Prod Res* 2014;**16**:891–900.
37. Jiang ZB, Meng XH, Jiang BY, Zhu CG, Guo QL, Wang SJ, et al. Two 2-(quinonylcarboxamino)benzoates from the lateral roots of *Aconitum carmichaelii*. *Chin Chem Lett* 2015;**26**:653–6.
38. Meng XH, Jiang ZB, Zhu CG, Guo QL, Xu CB, Shi JG. Napelline-type C_{20}-diterpenoid alkaloid iminiums from an aqueous extract of "fu zi": solvent-/base-/acid-dependent transformation and equilibration between alcohol iminium and aza acetal forms. *Chin Chem Lett* 2016;**27**:993–1003.
39. Meng XH, Jiang ZB, Guo QL, Shi JG. A minor arcutine-type C_{20}-diterpenoid alkaloid iminium constituent of "fu zi". *Chin Chem Lett* 2017;**28**:588–92.
40. Guo Q, Wang Y, Lin S, Zhu C, Chen M, Jiang Z, et al. 4-Hydroxybenzyl-substituted amino acid derivatives from *Gastrodia elata*. *Acta Pharm Sin B* 2015;**5**:350–7.
41. Guo QL, Wang YN, Zhu CG, Chen MH, Jiang ZB, Chen NH, et al. 4-Hydroxybenzyl-substituted glutathione derivatives from *Gastrodia elata*. *J Asian Nat Prod Res* 2015;**17**:439–54.
42. He J, Luo Z, Huang L, He J, Chen Y, Rong X, et al. Ambient mass spectrometry imaging metabolomics method provides novel insights into the action mechanism of drug candidates. *Anal Chem* 2015;**87**:5372–9.
43. Guo QL, Lin S, Wang YN, Zhu CG, Xu CB, Shi JG. Gastrolatathioneine, an unusual ergothioneine derivative from an aqueous extract of

"tian ma": a natural product co-produced by plant and symbiotic fungus. *Chin Chem Lett* 2016;**27**:1577–81.
44. Liu Z, Wang W, Feng N, Wang L, Shi J, Wang X. Parishin C′s prevention A$\beta_{1\text{-}42}$-induced inhibition of long-term potentiation is related to NMDA receptors. *Acta Pharm Sin B* 2016;**6**:189–97.
45. Li DW, Guo QL, Meng XH, Zhu CG, Xu CB, Shi JG. Two pairs of unusual scalemic enantiomers from *Isatis indigotica* leaves. *Chin Chem Lett* 2016;**27**:1745–50.
46. Guo Q, Xia H, Shi G, Zhang T, Shi J. Aconicarmisulfonine A, a sulfonated C_{20}-diterpenoid alkaloid from the lateral roots of *Aconitum carmichaelii*. *Org Lett* 2018;**20**:816–9.
47. Guo Q, Xia H, Meng X, Shi G, Xu C, Zhu C, et al. C_{19}-Diterpenoid alkaloid arabinosides from an aqueous extract of the lateral root of *Aconitum carmichaelii* and their analgesic activities. *Acta Pharm Sin B* 2018;**8**:409–19.
48. Chen M, Gan L, Lin S, Wang X, Li L, Li Y, et al. Alkaloids from the root of *Isatis indigotica*. *J Nat Prod* 2012;**75**:1167–76.
49. Chen M, Lin S, Li L, Zhu C, Wang X, Wang Y, et al. Enantiomers of an indole alkaloid containing unusual dihydrothiopyran and 1,2,4-thiadiazole rings from the root of *Isatis indigotica*. *Org Lett* 2012;**14**:5668–71.
50. Wang XL, Chen MH, Wang F, Bu PB, Lin S, Zhu CG, et al. Chemical constituents from root of *Isatis indigotica*. *China J Chin Mater Med* 2013;**38**:1172–82.
51. Liu YF, Chen MH, Wang XL, Guo QL, Zhu CG, Lin S, et al. Antiviral enantiomers of a bisindole alkaloid with a new carbon skeleton from the roots of *Isatis indigotica*. *Chin Chem Lett* 2015;**26**:931–6.
52. Liu YF, Chen MH, Guo QL, Lin S, Xu CB, Jiang YP, et al. Antiviral glycosidic bisindole alkaloids from the roots of *Isatis indigotica*. *J Asian Nat Prod Res* 2015;**17**:689–704.
53. Liu YF, Chen MH, Lin S, Li YH, Zhang D, Jiang JD, et al. Indole alkaloid glucosides from the roots of *Isatis indigotica*. *J Asian Nat Prod Res* 2016;**18**:1–12.
54. Liu Y, Wang X, Chen M, Lin S, Li L, Shi J. Three pairs of alkaloid enantiomers from the root of *Isatis indigotica*. *Acta Pharm Sin B* 2016;**6**:141–7.
55. Chen MH, Lin S, Wang YN, Zhu CG, Li YH, Jiang JD, et al. Antiviral stereoisomers of 3,5-bis(2-hydroxybut-3-en-1-yl)-1,2,4-thiadiazole from the roots of *Isatis indigotica*. *Chin Chem Lett* 2016;**27**:643–8.
56. Liu Y, Chen M, Guo Q, Li Y, Jiang J, Shi J. Aromatic compounds from an aqueous extract of "ban lan gen" and their antiviral activities. *Acta Pharm Sin B* 2017;**7**:179–84.
57. Meng L, Guo Q, Liu Y, Chen M, Li Y, Jiang J, et al. Indole alkaloid sulfonic acids from an aqueous extract of *Isatis indigotica* roots and their antiviral activity. *Acta Pharm Sin B* 2017;**7**:334–41.
58. Meng LJ, Guo QL, Xu CB, Zhu CG, Liu YF, Chen MH, et al. Diglycosidic indole alkaloid derivatives from an aqueous extract of *Isatis indigotica* roots. *J Asian Nat Prod Res* 2017;**19**:529–40.
59. Meng L, Guo Q, Liu Y, Shi J. 8, 4′-Oxyneolignane glucosides from an aqueous extract of "ban lan gen" (*Isatis indigotica* root) and their absolute configurations. *Acta Pharm Sin B* 2017;**7**:638–46.
60. Meng LJ, Guo QL, Zhu CG, Xu CB, Shi JG. Isatindigodiphindoside, an alkaloid glycoside with a new diphenylpropylindole skeleton from the root of Isatis indigotica. *Chin Chem Lett* 2018;**29**:119–22.
61. Meng L, Guo Q, Chen M, Jiang J, Li Y, Shi J, Isatindolignanoside A. a glucosidic indole-ignan conjugate from an aqueous extract of the *Isatis indigotica* roots. *Chin Chem Lett* 2017. Available from: <http://dx.doi.org/10.1016/j.cclet.2017.12.001>.
62. Davision EK, Hume PA, Sperry J. Total synthesis of an *Isatis indigotica*-derived alkaloid using a biomimetic thio-Diels–Alder reaction. *Org Lett* 2018;**20**:3545–8.
63. Breitmaier E, Voelter W. In: *Carbon-13 NMR spectroscopy: high-resolution methods and applications in organic chemistry and biochemistry*. 3rd completely rev ed. New York: VCH; 1990, p. 115–6.
64. Nie L, Wang G, Dai Z, Lin R. Determination of epigoitrin and goitrin in *Isatidis Radix* by chiral high performance liquid chromatography. *Chin J Chromatogr* 2010;**28**:1001–4.
65. Hanschen FS, Lamy E, Schreiner M, Rohn S. Reactivity and stability of glucosinolates and their breakdown products in foods. *Angew Chem Int Ed Engl* 2014;**53**:11430–50.
66. He WY, Gao RM, Li XQ, Jiang JD, Li YH. *In vitro* anti-influenza virus activity of 10 traditional Chinese medicines. *Acta Pharm Sin* 2010;**45**:395–8.
67. Cheng W, Zhu C, Xu W, Fan X, Yang Y, Li Y, et al. Chemical constituents of the bark of *Machilus wangchiana* and their biological activities. *J Nat Prod* 2009;**72**:2145–52.